ELSEVIER

Journal of Photochemistry and Photobiology A: Chemistry 105 (1997) 235–248

Journal of PHOTOCHEMISTRY AND PHOTOBIOLOGY A:CHEMISTRY

Photomodulation of conformational states of p-phenylazobenzyloxycarbonyl-L-proline and related peptides [1]

S. Rudolph-Böhner [a], M. Krüger [a], D. Oesterhelt [a], L. Moroder [a,*], T. Nägele [b], J. Wachtveitl [b]

[a] *Max-Planck-Institut für Biochemie, D-82152 Martinsried, Germany*

[b] *Institut für Medizinische Optik, Ludwig-Maximilian-Universität München, München, Germany*

Received 11 September 1996; accepted 12 September 1996

Abstract

In linear flexible peptides the isomeric equilibria of aminoacyl-L-proline peptide bonds are known to be shifted in favor of the trans configuration, whereas in *N*-urethanyl-L-proline compounds the cis configuration is preferred with stabilization of a C_7 conformation, i.e. of an inverse γ-type turn. To analyze the effects of a photoswitchable configuration in the urethane moiety on this small ordered structure element the photochrome azobenzene was incorporated as a urethane group into proline and the proline peptides Pro–Phe and Pro–Phe–Gly. The p-phenylazobenzyloxycarbonyl compounds retain the preferred cis configuration of the C–N urethane bond and undergo a reversible photomodulated trans to cis isomerization of the azobenzene moiety with more or less pronounced effects on the distribution of the four possible isomers as detected by FTIR and NMR spectroscopy. Correspondingly, detectable changes in the population of the C_7 conformation were observed upon irradiation making this system highly promising for monitoring dynamics by time-resolved spectroscopy. © 1997 Elsevier Science S.A.

Keywords: *N*-urethanyl-L-proline compounds; Azobenzene derivatives; Photoisomerization; C_7 conformation; γ-type turn

1. Introduction

The large change in geometry and polarity of azobenzene resulting from its light-induced trans to cis isomerization [1] has extensively been exploited in the past for the design and synthesis of photoresponsive systems [2,3]. Among these, poly-α-amino acids, with a large number of built-in photochromic groups, allowed for modulating in reversible manner macromolecular conformations and physical properties and thus, for mimicking biological systems. Because of the intrinsic chemical heterogeneity of these copolymers only crude pictures of the dynamics of conformational transitions could be obtained whereas microenvironmental changes remained elusive. These, however, should become more easily detectable if azobenzene groups are placed into topochemically defined positions of peptide structures more or less restricted in their conformational space.[2]

Detailed spectroscopic and crystallographic studies on urethane-protected L-amino acids in the solid state and in solution have clearly revealed a preferred cis configuration about the C–N urethane bond [6–10]. This preference is even more pronounced in the case of *N*-urethanyl-L-Pro derivatives, whereas in linear flexible peptides the isomeric equilibria of aminoacyl-L-Pro peptide bonds are known to be shifted in favor of the trans configuration because of the sterical hindrance between the aminoacyl-Cα and the Pro-C$^{\delta}$ carbon atoms [11–13]. Vibrational CD and FTIR spectra in the CO stretching region of concentrated *N*-urethanyl-L-amino acid solutions are consistent with a conformational space of $\Phi = -60°$ to $-90°$ and $\Psi = +30°$ to $+90°$ for intermolecular hydrogen-bonded dimers of the cis isomers. Conversely, in dilute solution the spectral features indicate self-association of the cis isomer with formation of a seven-membered intramolecular ring closed by hydrogen bonding between the carboxyl group and the urethane oxygen in a

* Corresponding author.

[1] Presented at the International Meeting of Physical Chemistry on *Intra- and inter-molecular photoprocesses of conjugated molecules*, Riccione, Italy, July 14–18, 1996.

Abbreviations: Z, benzyloxycarbonyl; PZ, p-phenylazobenzyloxycarbonyl; DMSO, dimethylsulfoxide; FTIR, Fourier transform infrared spectroscopy; NMR, nuclear magnetic resonance; NOESY, nuclear overhauser enhancement spectroscopy; ROESY, rotating frame overhauser enhancement spectroscopy; HMQC, heteronuclear multiple quantum coherence; COSY, correlated spectroscopy; TOCSY, total correlated spectroscopy

[2] In the course of this work two studies with similar intentions have been reported [4,5].

PII S1010-6030(96)04497-8

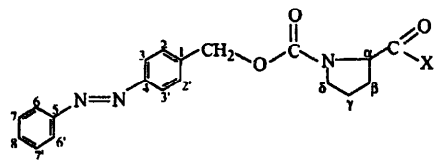

X = –OH
–Phe–OH
–Phe–Gly–OH

Fig. 1. Structure of the PZ compounds used in the present study.

restricted conformational space of $\Phi \sim -80°$ and $\Psi \sim +75°$ corresponding to an inverse γ-type turn [10]. These values of the dihedral angles are similar to those of a C_7 conformation, $(\Phi,\Psi) = (-80°, +80°)$, in peptides [14] that is characterized by a seven-membered intramolecular ring formed as result of hydrogen bonding between the carbonyl of the amino acid residue (i) and the NH hydrogen of residue ($i+2$). This C_7 conformation was shown to be energetically even more favored when proline represents residue $i+1$ [14]. We have selected this short ordered structural element of peptides and proteins to attempt its photomodulation by a built-in light switch and thus a monitoring of the dynamics of conformational transitions by time-resolved spectroscopy.

For this purpose the urethane derivative p-phenylazobenzyloxycarbonyl-L-proline (PZ-Pro-OH) was used which contains the proline residue with its high tendency for the C_7 fold and the photoswitchable azobenzene moiety in the urethane group. Moreover, PZ-Pro-OH was extended C-terminally to PZ-Pro–Phe-OH and Pz-Pro–Phe–Gly-OH (Fig. 1) to possibly stabilize peptide backbone C_7 structures, i.e. γ turns with the X-Pro bond in the trans configuration [14]. These simple model systems with the built-in photochrome should allow study of the possible effects of the photomodulated trans to cis isomerization of the azobenzene moiety on the configurational equilibria of the urethane C–N bond and thus, on the possible preferred conformations of these small-sized molecules.

2. Experimental

2.1. Materials

Reagents and solvents for synthesis and spectroscopy were of the highest quality commercially available. PZ-Pro-OH was synthesized by acylation of proline with p-phenylazobenzyl chloroformate as described previously [15]. Conversion of PZ-Pro-OH into the *N*-hydroxysuccinimide ester and subsequent reaction with H-Phe-OH or H-Phe–Gly-OH by conventional methods of peptide synthesis led to PZ-Pro–Phe-OH and PZ-Pro–Phe–Gly-OH as homogeneous and analytically well characterized compounds. Z-Pro-OH was prepared according to standard procedures.

2.2. Methods

2.2.1. UV difference spectroscopy

Spectra in the near-UV/vis region were recorded on a two-beam absorption spectrometer (Lambda 19, Perkin–Elmer) equipped with a deuterium lamp. Photoisomerization was induced by irradiation of the sample inside the spectrometer with light of the appropriate wavelength. A 1000 W Xe-lamp (LOT Oriel, Germany) was used as a light source, since the spectrum of this lamp contained all desired wavelengths in sufficient intensity. The light was passed through a 4 cm water cuvette and an interference filter ($\lambda_{max} = 435$ nm or 340 nm) or a reflection filter ($\lambda_{max} = 260$ nm). The spectrally selected light was focused onto a quartz lightguide which was mounted in the spectrometer to allow an optimal irradiation of the sample. A shutter was placed between the filters and the lightguide to allow an exact control of the irradiation conditions. A power meter (Newport, USA) was used to determine the light intensity at the probe site. For the trans to cis photoisomerization of the azobenzene (irradiation at 340 nm) the intensity was adjusted to 0.3 mW cm^{-2} and absorption spectra of the irradiated samples were recorded every 30 s. With this set-up it is possible to determine the quantum yield of the photoisomerization.

2.2.2. Time-resolved spectroscopy

The transient absorbance changes were recorded in pump-and-probe experiments using light pulses generated by a Ti:Sapphire oscillator/regenerative amplifier system operating at a wavelength of 870 nm, which is described in detail elsewhere [16]. The frequency of the light pulses was doubled in a non-linear LBO crystal and then split into two parts. One part was used directly to excite the sample, the second part was focused in a water cuvette where a white light continuum was generated that provided tunable probe pulses. The instrumental response function was between 180 fs and 250 fs throughout the entire observed spectral range.

The transient absorption dynamics of PZ-Pro-OH and PZ-Pro–Phe–Gly-OH in ethanol was analyzed in the wavelength region between 350 nm and 490 nm following an excitation pulse at 435 nm. The samples were preilluminated to prepare a sufficient amount of *cis*-PZ isomer absorbing at 435 nm. Fast pumping assured a complete exchange of the sample between the laser shots. The polarization between pump and probe pulse is 54.7° (magic angle) in all experiments. For delay times up to 1 ps linear scaling was used, for longer times the scaling was logarithmic. The experimental data were fit by a sum of exponential functions convoluted with the instrumental response function.

2.2.3. Analytical chromatography

HPLC was carried out with Waters equipment (Eschborn, Germany) on Nucleosil 300/C8 (Machery and Nagel, Düren, Germany) using a linear gradient of acetonitrile/2% H_3PO_4 from 5:95 to 80:20 in 30 min (UV monitoring at 214 nm).

2.2.4. IR spectroscopy

The FTIR spectra were recorded on a Perkin–Elmer 1760X FTIR spectrometer equipped with a Fast Recovery DTGS detector. For each spectrum 128 interferograms at 4 cm^{-1} resolution were collected at room temperature and apodized with a triangular function. To minimize the disturbing influence of water vapour in the amide I region the spectrometer was continuously purged with nitrogen. As criterion for the complete water vapour subtraction the obtainment of a straight base line from 2000 to 1750 cm^{-1} was used [17,18]. Samples were dissolved in DMSO-d_6 at 50 mmol concentration and spectra were recorded with an ATR cell consisting of a microrod circle crystal of ZnSe 1/8″ (Spectra-Tech Inc., USA). Each spectrum was subtracted for the solvent before and after irradiation whereby particular attention was paid to operate with both the sample and the reference solution under strictly identical conditions. Without this correction with a reference solution a large band of water in DMSO covering the amide I region is observed. Deconvolution of the spectra was performed with the Peak Separation and Analysis Programme "Peak Fit" for Windows of Jandel Scientific (Erkrath, Germany). The frequencies of the band centers obtained by second-derivitization of the spectra as well as known IR band assignments of similar compounds [11] were used as initial input parameters for the band-fitting procedure. We found empirically that the spectra are fitted reasonably well assuming Gaussian line shapes for the single components. The procedure applied is essentially that reported by Byler and Susi [19] and consists of a least-squares minimization with a maximum of 500 iteration steps.

2.2.5. NMR spectroscopy

Homonuclear (500.13 MHz) and heteronuclear (125.76 MHz) NMR spectra of the PZ compounds prior and after irradiation were recorded in DMSO-d_6 (30–50 mM) using Bruker AM500 and Bruker AMX500. For 1D and 2D spectra of PZ-Pro-OH the following parameters were used; 1D-^{1}H-NMR: 32 acquisitions, size 32 K, sweep width 8333.3 Hz; COSY [20]: size 1 K, sweep width 5268.1 Hz in t1 and t2, 64 acquisitions, 512 increments (TPPI [21]); NOESY [22,23]: mixing time 800 ms, size 2 K, sweep width 6250.0 Hz in t1 and t2, 32 acquisitions, 492 increments (TPPI); HMQC [24]: garp-decoupling during acquisition, size 2 K, 512 increments (TPPI), 64 acquisitions, 5208.3 Hz in t2 and 30 000 Hz in t1. For PZ-Pro–Phe-OH; 1D-^{1}H-NMR: 32 acquisitions, size 32 K, sweep width 8333.3 Hz; ROESY [25,26]: 100 ms spin-lock, 64 acquisitions, size 2 K, 600 increments (TPPI), spin-lock power 4 kHz, sweep width 5263.1 Hz in t1 and t2. For PZ-Pro–Phe–Gly-OH; 1D-^{1}H-NMR: 32 acquisitions, size 32 K, sweep width 8333.3 Hz; TOCSY [27,28]: mixing time for MLEV17 49 ms, size 2 K, sweep width 5263.1 Hz in t1 and t2, 8 acquisitions, 256 increments; HMQC: garp-decoupling during acquisition, size 2K, 256 increments (TPPI), 32 acquisitions, 5208.3 Hz in t2 and 30 000 Hz in t1; ROESY: 100 ms spin-lock, 96 acquisitions, size 2 K, 800 increments (TPPI), spin-lock power 4 kHz, sweep width 5263.1 Hz in t1 and t2; prior to transformation of the TOCSY, NOESY and ROESY spectra gaussian window function in t2 and shifted sine-bell function in t1 were used; prior to transformation of the COSY and HMQC spectra sine-bell functions in both dimensions were applied. Temperature dependence of the amide protons of PZ-Pro–Phe-OH and PZ-Pro–Phe–Gly-OH, and of the CHα resonances of PZ-Pro-OH were measured at 500.13 MHz taking nine spectra of each compound after irradiation (4 h) between 300 K and 320 K with 32 acquisitions, sweep width of 7575.7 Hz and 32 K. 1D ^{13}C-{^{1}H} spectra of the three PZ compounds before and after irradiation were recorded at 100.614 MHz in DMSO-d_6 (30–50 mM) using Bruker AM400 and the following parameters: CPD decoupling, size 32 K, relaxation delay 1 s, 964 (PZ-Pro-OH), 1200 (PZ-Pro–Phe-OH), 2800 (PZ-Pro–Phe–Gly-OH) acquisitions, sweep width 27 777 Hz. The NMR spectra recorded on AMX500 were transformed with XWINNMR 1.0 and 1.1 on a Silicon Graphics IRIS Indigo R4000. Nomenclature of the chemical shifts of Tables 2, 4 and 5 for the azobenzene moiety is according to Fig. 1.

For the FTIR and NMR measurements the PZ compounds in DMSO-d_6 were irradiated in quartz cells (2 mm) or NMR tubes (ϕ, 5 mm) at 366 nm with a UV lamp (0.8 mW cm^{-2}) at room temperature for periods of time indicated in the single experiments.

2.2.6. Computational procedures

Energy minimizations and molecular dynamics calculations using the cvff forcefield were performed on a IRIS Indigo R4000 with the Biosym program packages INSIGHTII 2.0 and DISCOVER 95.0. The built-up starting structures of the four isomers of each compound were minimized using the 2000 steps optimization starting with the steepest descents, moving on to conjugate gradients and finishing with the BFGS algorithm. The total energies (kcal mol^{-1}) including van der Waals and Coulomb contributions of the single isomers of each PZ compound could be monitored. For converting the *trans*-azo-*cis*-Pro isomer into the *trans*-azo-*trans*-Pro isomer molecular dynamics simulation was performed using 10 ps dynamics with a force constant of 400 kcal mol^{-1} $Å^{-2}$ and 1 ps equilibration.

3. Results

3.1. Configurational and conformational characterization of PZ-Pro-OH

Isomerization of azobenzene is known to be significantly affected by location and nature of substituents [29]. The $\pi\pi^*$ absorption maximum of non-irradiated PZ-Pro-OH is centered at 323 nm (Fig. 2) and the $n\pi$ at 427 nm. UV measurements with irradiation at 340 nm and 435 nm, respectively, result in full reversibility of the cis ↔ trans isomerization of the PZ-Pro-OH system. A comparative analysis

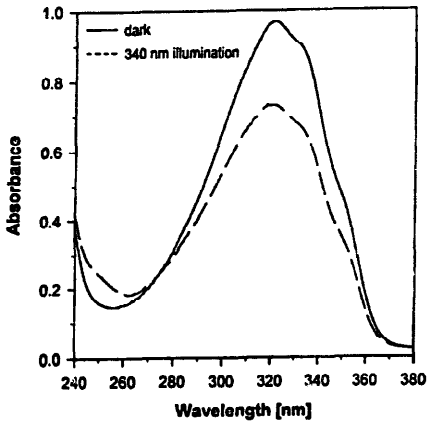

Fig. 2. UV spectra of PZ-Pro-OH before and after irradiation at 340 nm.

confirmed that the efficiency of the photoisomerization of PZ-Pro-OH was identical to that of azobenzene.

For the characterization of the system at configurational equilibrium, before and after irradiation, chromatographic procedures as well as FTIR and NMR spectroscopy were used. Irradiation was performed at 366 nm, i.e. not at the absorption maximum of the trans isomer (323 nm), but where in analogy to azobenzene the absorption of the cis isomer is expected to be minimal in order to achieve the highest *cis*-azo content in the photostationary experiments. After 3 h light exposure the HPLC elution profile of PZ-Pro-OH (data not shown) consists of two well separated double peaks which were assigned to the trans and cis isomer of the azobenzene moiety, whereas the double peak character was attributed to the cis/trans isomers of the X-Pro bond. Conversely, before irradiation mainly the not well resolved double peak of higher t_R value was observed indicating a large preference of the *trans*-azo isomer in the initial photostationary state in full agreement with the known photochromic properties of azobenzene derivatives. Quantification of the *cis/trans*-azo isomer ratio is difficult because of the unknown differences of the extinction coefficients in the far-UV. Similarly, quantification of the *cis/trans*-Pro isomers could not be achieved by this chromatographic procedure due to the poor resolution of the two isomers. Nevertheless, visual examination of the non-resolved double peak indicates a slight excess of one of the two *cis/trans*-Pro isomers and their almost equidistribution before and after irradiation. Thermal relaxation of the irradiated PZ-Pro-OH probes to the initial state in the dark at room temperature was found to be a very slow, but fully reversible process.

The band assignments of the FTIR spectra of Z-Pro-OH in the amide I region are known for $CHCl_3$ solutions, but only partly for DMSO solutions [10]. Therefore band assignments of the FTIR spectrum of Z-Pro-OH in DMSO were performed in analogy to the literature data of the $CHCl_3$ solution and then used to assign the bands of the FTIR spectrum of PZ-Pro-OH in DMSO (Table 1). The IR absorption bands of the azobenzene moiety in the 1500–1400 cm^{-1} region are weak and overlapped by the amide II absorption bands and other aromatic bands. Thus, exact assignments in this region are difficult; furthermore, the ATR technique applied in the measurements does not allow for quantifying the absorption intensities in this region. The aromatic absorption bands around 1600–1800 cm^{-1} are of weak intensities.

In the amide I region the urethane CO stretching band of non-hydrogen-bonded species consists of contributions at 1702 and 1707 cm^{-1} corresponding to the trans and cis isomer, respectively. Because of the unknown absolute intensities of these bands an exact quantification cannot be performed. The stronger band corresponding to the cis isomer, however, compares well with the known preference of *N*-urethanyl-L-proline derivatives for the cis configuration. Moreover, two additional urethane CO bands at 1690 and 1670 cm^{-1} are present which were assigned to the strongly and weakly hydrogen-bonded species, respectively. Since such hydrogen-bonded species should result from the C_7 conformation of the cis isomer [10], in the sum an excess of the *cis*-Pro isomer should be present at configurational equilibrium of the non-irradiated probe as previously reported for Z-Pro-OH [9,10].

The appearance of a rather strong band at 1725 cm^{-1} would suggest the presence of dimers at 50 mmol concentra-

Table 1
Band assignments of the FTIR spectra of Z-Pro-OH and PZ-Pro-OH in DMSO

Assignments	Z-Pro-OH (cm^{-1})	PZ-Pro-OH (cm^{-1})	PZ-Pro-OH after 170 min of irradiation (cm^{-1})	PZ-Pro-OH after 14 h of irradiation (cm^{-1})
Free carboxylic acid stretch	1762, weak	1754, weak	1759, weak	1753, very weak
			1744, medium	1744, weak
Intermolecular hydrogen-bonded urethane carbonyl stretch	1730, weak–medium	1725, strong	1724, strong	1725, strong
Free urethane carbonyl stretches of the cis and trans isomers	1702, strong	1702, strong	1702, strong	1702, strong
	1712, strong	1707, strong	1707, strong	1707, strong
Weakly hydrogen-bonded urethane carbonyl-stretching vibration	1693, medium	1690, medium	1692, medium	1691, medium
Strongly hydrogen-bonded urethane carbonyl stretch	1674, weak–medium	1670, weak	1670, weak	1665, medium
			1636, very weak	1628, weak
Aromatic absorption bands	1608, very weak	1605, very weak	1605, very weak	1603, weak
	1587, very weak	1584, very weak	1582, very weak	1583, weak
	1575, very weak			

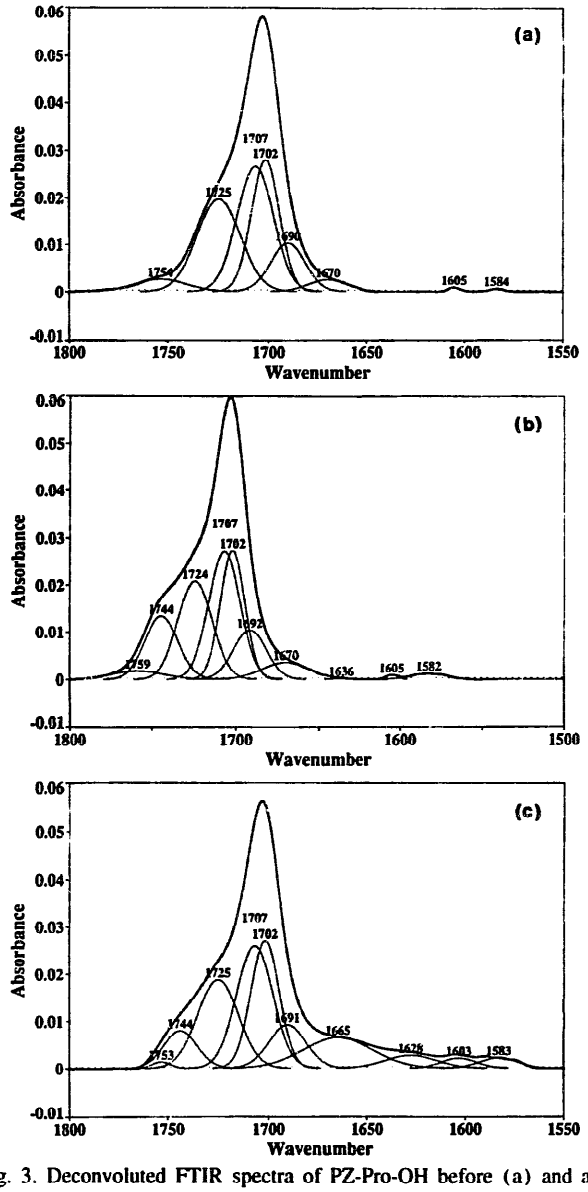

Fig. 3. Deconvoluted FTIR spectra of PZ-Pro-OH before (a) and after irradiation at 366 nm for 3 h (b) and 14 h (c).

tion since this band has been assigned in the case of concentrated solutions of *N*-urethanyl-L-amino acids to intermolecular hydrogen-bonded carboxylic CO [10]. Conversely, only a low-intensity band was observed for the non-hydrogen-bonded carboxyl group at 1754 cm^{-1}.

After irradiation the intensity ratios of the bands at 1725, 1702, 1707 and 1690 cm^{-1} remain constant whereas the urethane CO stretching band of strongly hydrogen-bonded species (C_7 conformation) increases significantly in intensity suggesting a stabilization of this inverse γ-type turn upon trans to cis isomerization of the azobenzene moiety (Fig. 3). Additionally, two new bands were detected in the irradiated state. The origin of these bands could not be exactly assigned, although their location is consistent with a hydrogen-bonded carboxyl group and a hydrogen-bonded urethane CO, respectively. These new absorption bands may possibly derive from hydrogen-bonded water adsorbed into the sample and thus, not subtractable with the reference solution. But it could also derive from a changed microenvironment of the urethane and carboxyl CO upon trans to cis isomerisation of the azobenzene group.

The ^1H and ^{13}C NMR spectrum of PZ-Pro-OH in DMSO-d_6 in the initial state exhibits mainly two sets of resonances which in view of the HPLC results (almost pure *trans*-azo isomer) were attributed to the two *cis*/*trans*-Pro isomers. Assignment of the resonances of these two isomers were achieved by 2D COSY and HMQC experiments. Since the classical assignment procedure of the configuration of X-Pro bonds via NOESY spectra was prevented in the urethane-type proline derivative because of the absence of a Cα proton, the resonances were assigned on the basis of the chemical shifts [30–32] of the *cis*/*trans* Cβ and Cγ carbons as well as of those of the Cα and Cδ carbons (Table 2). Upon irradiation, trans to cis isomerization of the azobenzene moiety leads to two new sets of resonances as shown in Fig. 4. Thereby the resonances of the aromatic protons of the *cis*-azo isomers are shifted to higher field (Table 2). The intensity of the resonances related to the single isomers allowed their quantification both in the initial and irradiated state (Table 3). The high preference of PZ-Pro-OH for the *trans*-azo state (97%) before irradiation corresponds to its chromatographic behaviour. A comparative spectroscopic study on different *N*-urethanyl-proline derivatives like Z-Pro-OH, Boc–Pro-OH and Aoc–Pro-OH revealed high contents of the cis isomer and no detectable effect of the nature of the urethane group on the *cis*/*trans* isomer ratio [9,10]. Rather surprising was, therefore, the *cis*/*trans*-Pro ratio of nearly 1, i.e. 53:47, for PZ-Pro-OH.

Irradiation of the PZ-Pro-OH solution in DMSO in a 2 mm quartz cell leads to trans to cis isomerization of the azobenzene moiety (*trans*/*cis*-azo isomer ratios: 47:53 after 3 h and 19:81 after 14 h as determined by NMR); but the *cis*/*trans*-Pro isomer distribution was not affected by this photoisomerization.

Temperature dependency of the resonances of the four isomers was expected to yield additional information about hydrogen bonding pattern, solvent accessibility and conformational stability. In the case of PZ-Pro-OH no amide protons are present, but the chemical shifts of the CHα protons of the *trans*-Pro isomers with the azobenzene moiety both in trans and cis configuration were found to be more affected by the temperature than in the case of the two *cis*-Pro isomers. The CHα protons of the *trans*- and *cis*-azo, *trans*-Pro isomers are shifted by 0.02 ppm to lower field raising the temperature from 300 K to 320 K, whereas the CHα proton of *trans*-azo, *cis*-Pro isomer and *cis*-azo, *cis*-Pro is shifted only by 0.006 ppm and 0.004 ppm, respectively.

3.2. Configurational and conformational characterization of PZ-Pro–Phe-OH and PZ-Pro–Phe–Gly-OH

Again the ^1H and ^{13}C NMR spectra of PZ-Pro–Phe-OH and PZ-Pro–Phe–Gly-OH in DMSO-d_6 were found to exhibit

Table 2
^{1}H, ^{13}C chemical shifts and coupling constants of PZ-Pro-OH in DMSO-d_6

Residue	^{1}H	^{1}H chemical shift (ppm)	Coupling constants (Hz)	^{13}C	^{13}C chemical shift (ppm)
trans-azo, *cis trans*-Pro before irradiation					
PZ1				*trans*-azo	122.5, 127.9, 128.2,
	trans-azo	7.92–7.84		C1, C2, 2',	129.5, 131.5, 140.6,
	H3, 3'	m, 4H		C3, 3' C4,	151.4, 151.3, 151.9
	H6, 6'			C5, C6, 6'	
				C7, 7', C8	
	trans-azo	7.64–7.49			
	H2, 2'	m, 5H			
	H7, 7'				
	H8				
				CH_2–O	65.3
	CH_2–O	5.19, s, 2H		*trans*-azo-	
	trans-azo	5.21, d, 1H	$J=13.6$	*cis, trans*-	
	cis trans-Pro	5, 11, d, 1H	$J=13.6$	Pro	
				CO	153.5
Pro 2	NH	–	–		–
	–COOH	12.65, br			
	α-CH			Cα	
	cis-Pro	4.29, dd	$J=3.5$, $J=9.0$	*cis*	58.4
	trans-Pro	4.19, dd	$J=3.2$, $J=8.7$	*trans*	59.0
	β-CH_2	2.31–2.16, m, β1		Cβ	
		1.98–1.79, m, β2		*cis*	30.4
				trans	29.4
	γ-CH_2	1.98–1.79, m		Cγ	
				cis	23.0
				trans	23.9
	δ-CH_2	3.53–3.37, m		Cδ	
				cis	46.8
				trans	46.2
				COOH	173.5
					173.9
trans, cis-azo-*cis, trans*-Pro after irradiation, 366 nm, 3 h					
PZ 1	*trans*-azo	7.92–7.84, m, 4H		*trans*/*cis*-azo	119.8, 120.0,
					120.1, 122.5,
	cis-azo	6.88–6.80, m, 4H		C1, C2, 2',	127.2, 127.7,
	H3, 3'			C3, 3', C4,	127.9, 128.2,
	H6, 6'			C5, C6, 6',	128.9, 129.5,
				C7, 7', C8,	131.6, 140.6,
					151.9, 152.8
	trans-azo	7.64–7.49, m, 5H			
	cis-azo	7.35–7.14, m, 5H			
	H2, 2'				
	H7, 7', H8				
	CH_2–O			CH_2–O	
	trans-	5.19, s, 2H	$J=13.6$	*trans, cis*-azo	65.2
	azo, *cis*	5.21, d, 1H	$J=13.6$	azo,	65.4
	trans-Pro	5.11, d, 1H		*cis trans*-Pro	
	cis-azo, *cis*,	5.02, s, 2H	$J=13.7$		
	trans-Pro	5.02, d, 1H	$J=13.7$		
		4.96, d, 1H			
				CO	153.2, 153.4
Pro 2	NH	–	–		153.6, 153.8
	–COOH	12.65, br			
	α-CH			Cα	
	trans-azo,			*cis*	58.5
	cis-Pro	4.29, dd	$J=3.5$	*trans*	59.0
			$J=9.0$		
	trans-Pro	4.19, dd	$J=3.2$,		
			$J=8.7$		

(continued)

Table 2 (*continued*)

Residue	^{1}H	^{1}H chemical shift (ppm)	Coupling constants (Hz)	^{13}C	^{13}C chemical shift (ppm)
	cis-azo, *cis*-Pro	4.23, dd	$J=3.7$, $J=8.7$		
	trans-Pro	4.15, dd	$J=3.6$, $J=8.4$		
	β-CH_2	2.29–2.12, m, β1		Cβ	
	trans cis-azo-*cis* *trans*-Pro	1.98–1.74, m, β2		*cis* *trans*	30.4 29.3
	γ-CH_2	1.98–1.74, m		Cγ	
	trans cis-azo-*cis* *trans*-Pro			*cis* *trans*	23.0 23.9
	δ-CH_2	3.53–3.35, m		Cδ	
	trans cis-azo-*cis* *trans*-Pro			*cis* *trans*	46.8 46.2
				COOH	173.6 173.9

mainly two sets of resonances in the initial state. 2D TOCSY and HMQC experiments were used to assign the resonances which are listed for the single isomers in Tables 4 and 5. ROESY spectra of both PZ compounds again did not allow for the *cis*/*trans*-Pro assignments, but these could be performed in analogy to the PZ-Pro-OH compound. Quantification of the isomeric states revealed for the di- and tripeptide derivatives before irradiation a *trans*-azo percentage of 97% (Tables 6 and 7). This result indicates that the C-terminal modifications do not affect the *trans*/*cis*-azo equilibrium in the initial photostationary state. After irradiation under identical conditions as PZ-Pro-OH (3 h) significantly higher contents of the *cis*-azo isomer were detected, i.e. 60% for PZ-Pro–Phe-OH and 76% for PZ-Pro–Phe–Gly-OH, suggesting a remarkable stabilization of this configurational state by the C-terminal extensions. Interestingly, even the *cis*/*trans*-Pro isomeric equilibria in the initial state were affected in comparison with that of PZ-Pro-OH, with a sig-

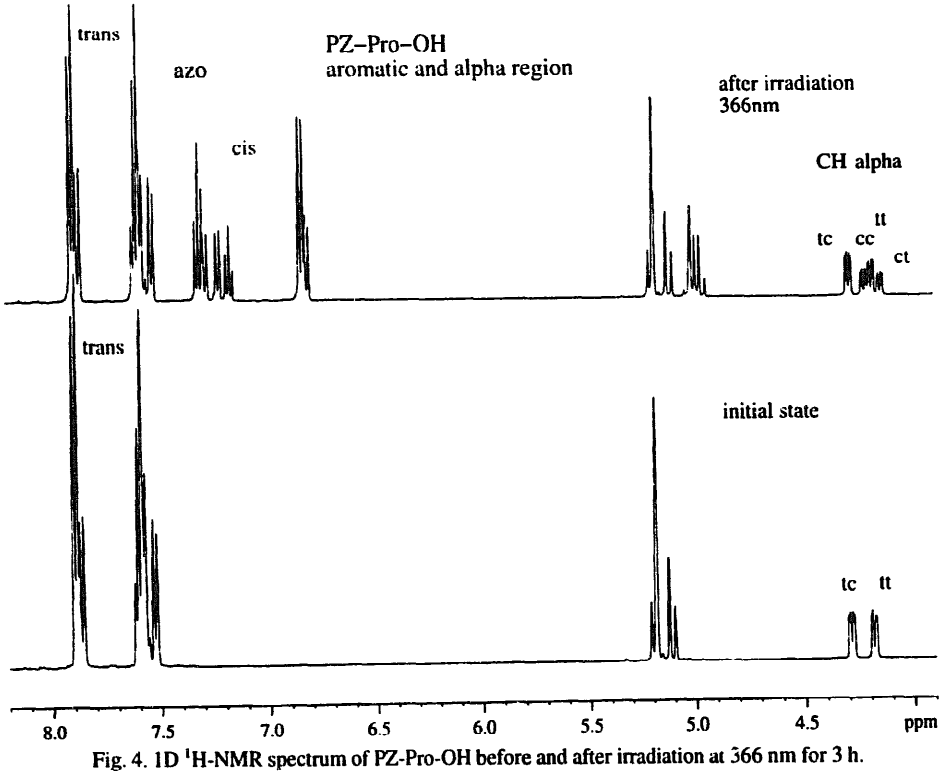

Fig. 4. 1D ^{1}H-NMR spectrum of PZ-Pro-OH before and after irradiation at 366 nm for 3 h.

nificant shift in favor of the *cis*-Pro isomer in the dipeptide derivative whereas in PZ-Pro–Phe–Gly-OH this preference is again partly annealed. Most interestingly, in the case of PZ-Pro–Phe-OH the light-induced trans to cis isomerization of the azobenzene moiety is accompanied by a detectable increase of the *trans*-Pro content (Table 6). The presence of a C_7 conformation in the dipeptide derivative similar to that in peptides or proteins would imply a ring closure by –C=O···H–N– hydrogen bonding with both amides in the trans configuration [14]. Induction and stabilization of this C_7 structure at conformational equilibrium could possibly derive from the *cis*-azo configuration.

In the tripeptide derivative PZ-Pro–Phe–Gly-OH (see Table 7) irradiation leads to inversion of the *cis*/*trans*-Pro ratio in the *trans*-azo isomer, a fact which can reasonably be explained only by a preferred isomerization of the *cis*-Pro isomer to the cis configuration of the azobenzene group. Decisive NMR evidence for explaining this phenomenon could not be obtained.

The chemical shifts of the NH Phe protons of the four isomers of PZ-Pro–Phe-OH are all high field-shifted by about 0.1 ppm raising the temperature from 300 K to 320 K. However, in the case of the *cis*-azo, *trans*-Pro isomer this effect is less pronounced than for the other three isomers. A temperature raise in the case of PZ-Pro–Phe–Gly-OH leads to a stronger shift of the amide protons than that observed for the PZ-Pro–Phe-OH isomers, but also to full overlapping, thus preventing assignments.

3.3. Time-resolved spectroscopy

The transient absorbance changes of PZ-Pro-OH and PZ-Pro–Phe–Gly-OH are shown in Fig. 5. The curves were recorded at two spectral regions which are dominated by the $\pi \rightarrow \pi^*$ transition of the trans isomer of the azobenzene moiety and the weaker $n \rightarrow \pi^*$ transition of its cis isomer, respectively. The dominant feature at early delay times is a strong induced absorption which disappears after less than 200 fs. If this component is interpreted as excited state absorption,

Table 3
PZ-Pro-OH in DMSO-d_6 at 300 K

Before irradiation		
	trans-azo 97%	*cis*-azo < 3%
trans-Pro	1, 46%	3 [a]
cis-Pro	2, 51%	4 [a]
trans:*cis*-Pro ratio	47:53	[a]
After irradiation 366 nm		
	trans-azo 54%	*cis*-azo 46%
trans-Pro	1, 24%	3, 21%
cis-Pro	2, 29%	4, 26%
trans:*cis*-Pro ratio	47:53	47:53

[a] Quantification is not possible. **1**, *trans*-azo, *trans*-Pro-OH (tt); **2**, *trans*-azo, *cis*-Pro-OH (tc); **3**, *cis*-azo, *trans*-Pro-OH (ct); **4**, *cis*-azo, *cis*-Pro-OH (cc).

the rapid decay is indicative for a population of the cis and trans ground states. These ground state bands show a further temporal evolution caused by orientational and cooling effects. The absorption changes at delay times longer than 50 ps are consistent with the steady state difference spectrum. The quantum yield and reaction dynamics of the photoproduct formation in the PZ peptide compounds compare well to the isomerization properties of azobenzene [33]. The experiments therefore demonstrate the high suitability of this system for the study of fast conformational changes.

4. Discussion

The spectroscopic data of PZ-Pro-OH confirm the results of previous studies on *N*-urethanyl-proline derivatives. The preference for the *cis*-Pro configuration is retained although to a lower extent with formation of the intramolecular hydrogen-bonded C_7 conformation. This local structure is apparently stabilized by the trans to cis isomerization of the azobenzene moiety as suggested by the comparative analysis

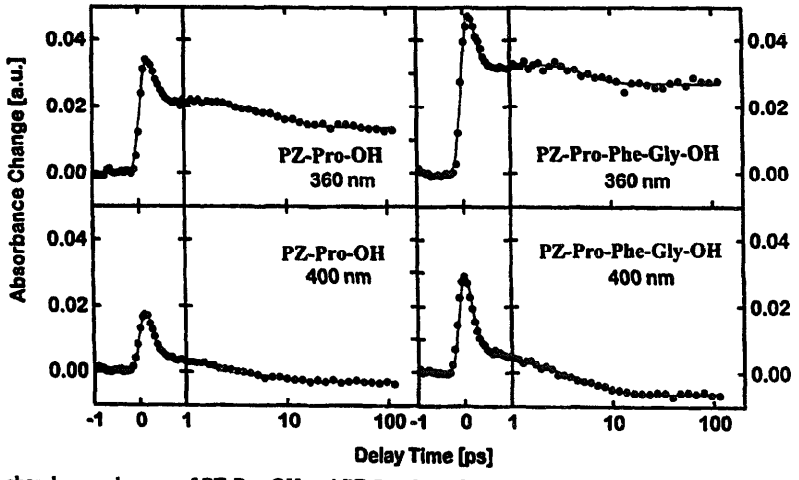

Fig. 5. Transient absorbance changes of PZ-Pro-OH and PZ-Pro–Phe–Gly-OH as monitored by time-resolved UV spectroscopy.

Table 4
^{1}H, ^{13}C chemical shifts and coupling constants of PZ-Pro–Phe-OH in DMSO-d_6

Residue	^{1}H	^{1}H chemical shift (ppm)	Coupling constants (Hz)	^{13}C	^{13}C chemical shift (ppm)
trans-azo, *cis trans*-Pro before irradiation					
PZ 1				*trans*-azo	122.4, 122.5, 127.8,
	trans-azo	7.88–7,82		C1, C2, 2′	128.2, 129.5, 131.5,
	H3, 3′	m, 4H		C3, 3′, C4,	140.7, 151.2, 151.4,
	H6, 6′			C5, C6, 6′	151.9
				C7, 7′, C8	
	trans-azo	7.62–7.55			
	H2, 2′	m, 5H			
	H7, 7′				
	H8				
	CH_2–O			CH_2–O	
	trans-azo,			*trans*-azo,	65.2, 65.3
	trans-Pro	5.20, d, 1H	$J=14.4$	*cis trans*-Pro	
		5.15, d, 1H	$J=14.4$	Pro	
	cis-Pro	5.06, d, 1H	$J=13.8$		
		5.00, d, 1H	$J=13.8$		
				CO	153.7
Pro 2	NH	–	–		–
	α-CH	4.30–4.22, m. 2H		Cα	
	cis-Pro		$J=3.5$, $J=9.0$	*cis*	59.3
	trans-Pro		$J=3.2$, $J=8.7$	*trans*	59.7
	β-CH_2	2.16–1.98, m, β1		Cβ	
		1.82–1.66, m, β2		*cis*	31.0
				trans	29.7
	γ-CH_2	1.82–1.66, m		Cγ	
				cis	22.8
				trans	23.6
	δ-CH_2	3.51–3.38, m		Cδ	
				cis	47.1
				trans	46.5
				CO	171.8
					172.1
Phe 2	NH				
	cis-Pro	8.24, d 1H	$J=8.7$		
	trans-Pro	8.10, d, 1H	$J=7.7$		
	H2, H2′	7.26–7.10, m, 5H			126.3, 128.0, 129.0,
	H3, H3′				129.2, 137.6
	H4				
	α-CH			Cα	
	cis-Pro	4.49, m, 1H		*cis*	53.2
	trans-Pro	4,44, m, 1H		*trans*	53.4
	β-CH_2	3.08–3.00, m, β1		Cβ	36.5
		2.97–2.95, m, β2		*cis*	
				trans	
	COOH	12.68, br		COOH	172.7
					172.9
trans cis-azo, *cis trans*-Pro after irradiation, 366 nm, 3 h					
PZ 1	*trans*-azo	7.88–7.82 m, 4H		*trans cis*-	119.7, 119.9,
				azo	122.4, 122.5,
	cis-azo	6.87–6.73, m, 4H		C1, C2, 2′,	127.0, 127.1,
	H3, 3′			C3, 3′, C4,	127.7, 129,4
	H6, 6′			C5, C6, 6′,	131.5, 140.6,
				C7, 7′, C8	151.2, 151.9
	trans-azo	7.62–755, m, 5H			
	cis-azo	7.34–7.02, m, 5H			
	H2, 2′				
	H7, 7′, H8				

(continued)

Table 4 (*continued*)

Residue	^{1}H	^{1}H chemical shift (ppm)	Coupling constants (Hz)	^{13}C	^{13}C chemical shift (ppm)
	trans-azo, *trans*-Pro	5.20, d, 1H	J=13.5	*trans cis*-azo	64.9
		5.15, d, 1H	J=13.5	*cis trans*-Pro	65.1
	cis-Pro	5.06, d, 1H	J=13.8	CH_2–O	65.2
		5.00, d, 1H	J=13.8		
	CH_2–O *cis*-azo, *trans*-Pro,	4.97, d, 1H	J=13.2		
		5.02, d, 1H	J=13.2		
	cis-Pro	5.00, d, 1H	J=13.2		
		5.05, d, 1H	J=13.2		
				CO	153.6
Pro 2	NH	–	–		–
	α-CH, *trans*-azo-*cis*, *trans*-Pro	4.29–4.23, m, 2H		Cα *cis* *trans*	59.3 59.7
	cis-azo-*cis*, *trans*-Pro	4.22–4.18, m, 2H			
	β-CH_2	2.15–1.94, m, β1		Cβ	
	trans, *cis*-azo-*cis*, *trans*-Pro	1.82–1.62, m, β2		*cis* *trans*	30.9 29.6
	γ-CH_2	1.82–1.62, m		Cγ	
	trans, *cis*-azo-*cis* *trans*-Pro			*cis* *trans*	22.7 23.6
	δ-CH_2	3.51–3.39, m		Cδ	
	trans, *cis*-azo-*cis*, *trans*-Pro			*cis* *trans*	47.0 46.4
				CO	172.1 172.0
Phe 2	NH				
	trans-azo-*cis*-Pro	8.24, d, 1H	J=8.7 J=7.7		
	trans-Pro	8.10, d, 1H			
	cis-azo-*cis*-Pro	8.20, d, 1H	J=8.3		
	trans-Pro	8.08, d, 1H	J=7.7		
	H2, H2' H3, H3' H4	7.34–7.02 m, 5H			126.2, 128.0, 128.9, 129.1, 137.5
	α-CH *trans*, *cis* *cis*, *trans*-Pro	4.29–4.23, m, 4H		Cα *cis* *trans*	53.2 53.3
	β-CH_2	3.07–2.98, m, β1 2.97–2.81, m, β2		Cβ *cis* *trans*	36.5
	COOH	12.68, br		COOH	172.7

of the FTIR spectra before and after irradiation. A comparison of the energies of the *trans*-azo, *cis*-Pro and *cis*-azo, *cis*-Pro isomers supports this conclusion. Furthermore, the temperature dependency of the chemical shifts of the CHα protons is indicative of more stable conformations for the two *cis*-Pro isomers than for the two *trans*-Pro isomers.

The surprisingly higher tendency of the C-terminally extended PZ-Pro compounds to light-induced trans to cis isomerization of the photochrome can only be attributed to a conformational effect of the peptide moiety. Energy minimizations and molecular dynamics calculations performed on the single isomers in vacuo and a comparison of the ener-

Table 5
^1H, ^{13}C chemical shifts and coupling constants of PZ-Pr–PHe–Gly-OH in DMSO-d_6

Residue	^1H	^1H chemical shift (ppm)	Coupling constants (Hz)	^{13}C	^{13}C chemical shift (ppm)
trans-azo-*cis*, *trans*-Pro before irradiation					
PZ1				*trans*-azo	122.4, 122.5, 127.7,
	trans-azo	7.89–7,81		C1, C2,2′,	128.3, 129.5, 131.5,
	H3, 3′	m, 4H		C3, 3′, C4,	140.5, 140.7, 151.2,
	H6, 6′			C5, C6, 6′	151.9
				C7, 7′, C8	
	trans-azo	7.63–7.40			
	H2, 2′	m, 5H			
	H7, 7′				
	H8				
	CH_2–O			CH_2–O	
	trans-azo,			*trans*-azo,	65.1, 65.5
	trans-Pro	5.22, d, 1H	$J=13.5$	*cis trans*-	
		5.15, d, 1H	$J=13.5$	Pro	
	cis-Pro	5.03, d, 1H	$J=13.5$		
		4.98, d, 1H	$J=13.5$		
				CO	153.7
					154.4
Pro 2	NH	–	–		–
	α-CH			Cα	
	cis-Pro	4.25, dd, 1H	$J=2.9$, $J=9.3$	*cis*	60.2
	trans-Pro	4.12, dd, 1H	$J=2.6$, $J=8.7$	*trans*	59.4
	β-CH_2	2.13–1.93, m, β1		Cβ	
		1.79–1.62, m, β2		*cis*	31.0
				trans	29.6
	γ-CH_2	1.79–1.62, m		Cγ	
				cis	22.8
				trans	23.7
	δ-CH_2	3.51–3.37, m		Cδ	
				cis	47.6
				trans	46.5
				CO	171.0
					171.3
Phe 2	NH				
	cis-Pro	8.15, d, 1H	$J=8.0$		
	trans-Pro	8.04, d, 1H	$J=8.4$		
	H2, H2′	7.27–7.05, m, 5H			126.1, 127.9, 129.1,
	H3, H3′				129.2, 137.8
	H4				
	α-CH			Cα	53.5
	cis-Pro	4.62, m, 1H		*cis*	
	trans-Pro	4.55, m, 1H		*trans*	
	β-CH_2	3.09–2.99, m, β1		Cβ	
		2.85–2.80, m, β2		*cis*	37.4
				trans	37.1
				CO	171.5
Gly 3	NH				
	cis-Pro	8.25, t, 1H	$J=5.5$		
	trans-Pro	8.16, t, 1H	$J=5.2$		
	α-CH			Cα	40.7
	cis-Pro	3.75, d, 2H	$J=5.2$	*cis*	
	trans-Pro	3.77, d, 2H	$J=5.5$	*trans*	
	COOH	12.68		COOH	171.9
trans cis, azo-*cis trans*-Pro after irradiation, 366 nm, 3 h					
PZ 1	*trans*-azo	7.89–7.81 m, 4H		*trans cis*-	119.7, 119.9,
				azo	120.0, 122.4,
	cis-azo	6.83–6.76, m, 4H		C1, C2, 2′	122.5, 126.9,
	H3, 3′			C3, 3′ C4,	127.1, 127.7,
	H6, 6′			C5, C6, 6′,	129.4, 131.4,
				C7, 7′, C8	131.5, 137.8, 151.9

(continued)

Table 5 (*continued*)

Residue	^{1}H	^{1}H chemical shift (ppm)	Coupling constants (Hz)	^{13}C	^{13}C chemical shift (ppm)
	trans-azo	7.63–7.55, m, 5H			
	cis-azo	7.33–7.03, m, 5H			
	H2, 2'				
	H7, 7', H8				
	trans-azo,			*trans cis*-	
	trans-Pro	5.22, d, 1H	J=13.5	azo,	64.9
		5.15, d, 1H	J=13.5	*cis trans*-	65.1
	cis-Pro	5.03, d, 1H	J=13.5	Pro,	65.5
		4.98, d, 1H	J=13.5	CH_2–O	
	CH_2–O				
	cis-azo				
	trans-Pro,	4.97, d, 1H	J=13.1		
		5.04, d, 1H	J=13.1		
	cis-Pro	4.88, d, 1H	J=13.5		
		4.77, d, 1H	J=13.5		
				CO	153.7
					154.4
	NH	–	–		–
	α-CH			Cα	
	trans-azo,			*cis*	59.4
	cis-Pro	4.25, dd, 1H	J=2.9, J=9.3	*trans*	60.2
	trans-Pro	4.12, dd, 1H	J=2.6, J=8.7		
	cis-azo,				
	cis-Pro	4.18, dd, 1H	J=2.9, J=9.3		
	trans-Pro	4.12, dd, 1H	J=2.5, J=8.7		
	β-CH_2	2.12–1.90, m, β1		Cβ	
	trans cis-	1.77–1.58, m, β2		*cis*	31.0
	azo, *cis*			*trans*	29.5
	trans-Pro				
	γ-CH_2	1.77–1.58, m		Cγ	
	trans cis-			*cis*	22.7
	azo, *cis*			*trans*	23.6
	trans-Pro				
	δ-CH_2	3.51–3.39, m		Cδ	
	trans cis-			*cis*	47.1
	azo, *cis*			*trans*	46.5
	trans-Pro				
				COOH	171.2
					171.4
Phe 2	NH				
	trans-azo,				
	cis-Pro	8.15, d 1H	J=8.0		
	trans-Pro	8.04, d, 1H	J=8.4		
	cis-azo,				
	cis-Pro	8.10, d, 1H	J=8.7		
	trans-Pro	8.00, d, 1H	J=8.4		
	H2, H2'	7.33–7.03, m, 5H			126.1, 127.8, 129.0,
	H3, H3'				129.1, 137.7
	H4				
	α-CH			Cα	
	trans cis-	4.65–4.50, m, 4H		*cis*	53.4
	azo,			*trans*	53.5
	cis trans-Pro				
	β-CH_2	3.12–2.94, m, β1		Cβ	
		2.88–2.74, m, β2		*cis*	37.4
				trans	37.1
				CO	171.4
					171.6

(*continued*)

Table 5 (*continued*)

Residue	^{1}H	^{1}H chemical shift (ppm)	Coupling constants (Hz)	^{13}C	^{13}C chemical shift (ppm)
Gly 3	NH				
	trans-azo,				
	cis-Pro	8.25, t, 1H	J=5.5		
	trans-Pro	8.16, t, 1H	J=5.2		
	cis-azo-	8.22, t, 1H	J=5.5		
	cis-Pro	8.13, t, 1H	overlap		
	trans-Pro				
	α-CH			Cα	40.6
	trans-azo,			*cis*	
	cis-Pro	3.75, d, 2H	J=5.2	*trans*	
	trans-Pro	3.77, d, 2H	J=5.5		
	cis-azo-	3.73, d, 2H	J=5.5		
	cis-Pro	3.77, d, 2H	J=6.1		
	trans-Pro				
	COOH	12.68		COOH	171.9

Table 6
PZ-Pro–Phe-OH in DMSO-d_6 at 300 K

Before irradiation		
	trans-azo 97%	*cis*-azo < 3%
trans-Pro	**1**, 36%	**3** [a]
cis-Pro	**2**, 61%	**4** [a]
trans:*cis*-Pro ratio	37:63	[a]
After irradiation 366 nm		
	trans-azo 40%	*cis*-azo 60%
trans-Pro	**1**, 15%	**3**, 24%
cis-Pro	**2**, 25%	**4**, 36%
trans:*cis*-Pro ratio	37:63	41:59

[a] Quantification is not possible; **1**, *trans*-azo, *trans*-Pro (tt); **2**, *trans*-azo, *cis*-Pro (tc); **3**, *cis*-azo, *trans*-Pro (ct); **4**, *cis*-azo, *cis*-Pro (cc).

Table 7
PZ-Pro–Phe–Gly-OH in DMSO-d_6 at 300 K

Before irradiation		
	trans-azo 97%	*cis*-azo < 3%
trans-Pro	**1** 41%	**3** [a]
cis-Pro	**2** 56%	**4** [a]
trans:*cis*-Pro ratio	42:58	[a]
After irradiation 366 nm		
	trans-azo 24%	*cis*-azo 76%
trans-Pro	**1**, 12%	**3**, 33%
cis-Pro	**2**, 12%	**4**, 43%
trans:*cis*-Pro ratio	51:49	42:58

[a] quantification is not possible; **1**, *trans*-azo, *trans*-Pro (tt); **2**, *trans*-azo, *cis*-Pro (tc); **3**, *cis*-azo, *trans*-Pro (ct); **4**, *cis*-azo, *cis*-Pro (cc).

gies of the *cis*/*trans*-Pro pair of isomers of PZ-Pro-OH, PZ-Pro–Phe-OH and PZ-Pro–Phe–Gly-OH before and after irradiation leads to the following interesting observation: the *cis*-Pro isomer is the most favored configuration in the initial state (*trans*-azo) for all three compounds; in the irradiated state (*cis*-azo) the *cis*-Pro is energetically favored in the case of PZ-Pro-OH and PZ-Pro–Phe–Gly-OH, whereas in the case of PZ-Pro–Phe-OH the *trans*-Pro isomer exhibits the lower total energy. In this case trans to cis isomerization of the azobenzene moiety leads to an increase of the *trans*-Pro isomer content, whereas in the case of PZ-Pro–Phe–Gly-OH the experimental data compare well with a preferred trans to cis isomerization of the azobenzene moiety of the *cis*-Pro isomer. As shown in Fig. 6, in the isomer *cis*-azo, *trans*-Pro of PZ-Pro–Phe-OH a C_7 conformation (classical γ turn) centered on Pro is stabilized by the intramolecular hydrogen bond between the Phe NH and the urethane carbonyl and by an aromatic interaction between the Phe side chain and the azobenzene moiety. This hydrophobic collapse may possibly be responsible for the observed weaker temperature dependency of the Phe amide proton which becomes less solvent accessible. The *cis*-azo, *cis*-Pro isomer of PZ-Pro–Phe–Gly-OH, shown in Fig. 7, exhibits a hydrogen bonding pattern involving the Phe NH as donor and the urethane oxygen as acceptor

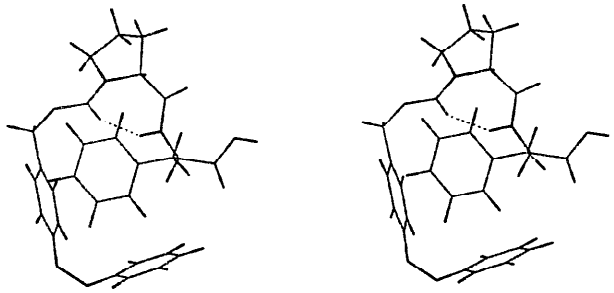

Fig. 6. Stereoview of the energy-minimized structure of the more populated PZ-Pro–Phe-OH isomer in the irradiated state (*cis*-azo, *trans*-Pro); $\Phi = +83.9°$ and $\Psi = -54.7°$ (classical γ turn, PZ CO···HN Phe).

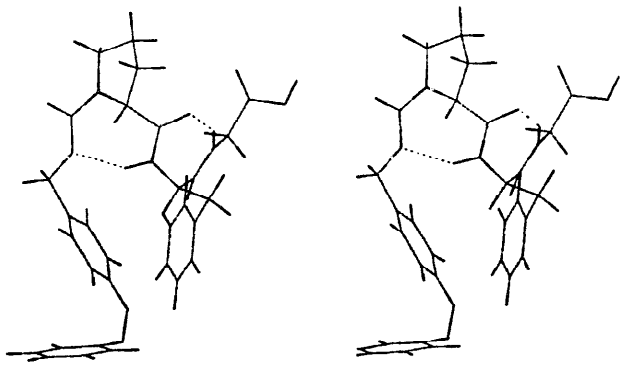

Fig. 7. Stereoview of the energy-minimized structure of the more populated configurational state of PZ-Pro-Phe-Gly-OH in the irradiated state (*cis*-azo, *cis*-Pro); $\Phi = -78.8°$ and $\Psi = +72.6°$ (inverse γ-type turn, PZ O···HN Phe), and $\Phi = +70.5°$ and $\Psi = -65.2°$ (classical γ turn, Pro CO···HN Gly).

(inverse γ-type turn with the urethane C–N bond in cis configuration), and the Gly NH and Pro CO (classical γ turn).

Since time-resolved UV spectroscopy clearly revealed that the PZ compounds are suitable for photomodulation of the cis↔trans isomerization of the azobenzene moiety on a femto- to picosecond time scale, related time-resolved IR spectroscopy could possibly allow for monitoring conformational transitions involving hydrogen bonds on a similar time scale.

References

[1] H. Rau, in H. Dürr and H. Bonas-Laurent (eds.), Studies in Organic Chemistry. Photochromism, Molecules and Systems, Vol. 40, Elsevier, Amsterdam, 1990, p. 165.
[2] O. Pieroni, A. Fissi and F. Ciardelli, J. Photochem. Photobiol., 44 (1986) 785.
[3] G.S. Kumar and D.C. Neckers, Chem. Rev., 89 (1989) 1915.
[4] L. Ulysse, J. Cubillos and J. Chmielewski, J. Am. Chem. Soc., 117 (1995) 8466.
[5] R. Cerpa, F.E. Cohen and I.D. Kuntz, Folding Design, 1 (1996) 91.
[6] E. Benedetti, B. Di Blasio, V. Pavone and C. Pedone, Biopolymers, 20 (1981) 1635.
[7] E. Benedetti, B. Di Blasio, V. Pavone, C. Pedone, C. Toniolo and G. Bonora, Int. J. Biol. Macromol., 2 (1980) 217.
[8] J.W. Bats, H. Fuess, H. Kessler and R. Schuck, Chem. Ber., 113 (1980) 520.
[9] E. Benedetti, A. Ciajolo, B. Di Blasio, V. Pavone, C. Pedone, C. Toniolo, C. and G.M. Bonora, Int. J. Peptide Protein Res., 14 (1979) 130.
[10] A.C. Chernovitz, T.B. Freedman and L.A. Nafie, Biopolymers, 26 (1987) 1879.
[11] C. Gratewohl and K. Wüthrich, Biopolymers, 15 (1976) 2025.
[12] C. Gratewohl and K. Wüthrich, Biopolymers, 15 (1976) 2043.
[13] J. Poznanski, A. Ejchart, K.L. Wierzchowski and M. Cuirak, Biopolymers, 33 (1993) 781.
[14] C. Toniolo, CRC Crit. Rev. Biochem., 10 (1980) 1.
[15] R. Schwyzer, P. Sieber and K. Zatsko, Helv. Chim. Acta, 41 (1958) 491.
[16] H. Huber, M. Meyer, T. Nägele, I. Hartl, H. Scheer, W. Zinth and J. Wachtveitl, Chem. Phys., 197 (1995) 297.
[17] D.L. Lee, P.I. Haris, D. Chapman and R.C. Mitchell, Biochemistry, 29 (1990) 9185.
[18] A. Dong, P. Huang and W.S. Caughy, Biochemistry, 29 (1990) 3303.
[19] D.M. Byler and H. Susi, Biopolymers, 25 (1986) 469.
[20] W.P. Aue, E. Bartholdi and R.R. Ernst, J. Chem. Phys., 64 (1976) 2229.
[21] D. Marion and K. Wüthrich, Biochem. Biophys. Res. Commun., 113 (1983) 967.
[22] J. Jeener, B. Meier, P. Bachmann and R.R. Ernst, J. Chem. Phys., 71 (1979) 4546.
[23] G. Bodenhausen, H. Kogler and R.R. Ernst, J. Magn. Reson., 58 (1984) 370.
[24] A. Bax and S. Subramanian, J. Magn. Reson., 67 (1986) 565.
[25] A. Bax and D.G. Davis, J. Magn. Reson., 63 (1985) 207.
[26] S.W. Fesik and E.R.P. Zuiderweg, J. Magn. Reson., 78 (1988) 588.
[27] A. Bax and D.G. Davis, J. Magn. Reson., 65 (1985) 355.
[28] L. Braunschweiler and R.R. Ernst, J. Magn. Reson., 53 (1983) 521.
[29] S.Jr. Lunak, M. Nepras, R. Hrdina and H. Mustroph, Chem. Phys., 184 (1994) 255.
[30] D.A. Torchia and F.A. Bovey, Macromolecules, 4 (1971) 246.
[31] D.E. Dorman, D.A. Torchia and F.A. Bovey, Macromolecules, 6 (1973) 80.
[32] W.E. Hull and H.R. Kricheldorf, Biopolymers, 19 (1980) 1103.
[33] J. Wachtveitl, T. Nägele, B. Puell, W. Zinth, M. Krüger, S. Rudolph-Böhner, D. Oesterhelt and L. Moroder, J. Photochem. Photobiol. A: Chem., 105 (1997) 283.